

## Excitation functions of $(p, \alpha)$ reactions on $^{64}\text{Ni}$ , $^{78}\text{Kr}$ , and $^{86}\text{Sr}$

S. M. Qaim,<sup>1</sup> M. Uhl,<sup>2,\*</sup> F. Rösch,<sup>1</sup> and F. Szelecsényi<sup>1,†</sup>

<sup>1</sup>*Institut für Nuklearchemie, Forschungszentrum Jülich GmbH, D-52425 Jülich, Germany*

<sup>2</sup>*Institut für Radiumforschung und Kernphysik, Universität Wien, A-1090 Vienna, Austria*

(Received 6 September 1994)

Excitation functions were measured by the stacked-foil technique for  $^{64}\text{Ni}(p, \alpha)^{61}\text{Co}$  and  $^{86}\text{Sr}(p, \alpha)^{83}\text{Rb}$  reactions from threshold up to 18.5 MeV. Thin samples of 95% enriched  $^{64}\text{Ni}$  were prepared by electrodeposition on gold foils, and those of 96.3% enriched  $^{86}\text{SrCO}_3$  via sedimentation on Cu backing. The radioactivity of the activation products was determined via high resolution  $\gamma$ -ray spectrometry. Statistical model calculations taking into account preequilibrium effects were performed for the experimentally measured competing reactions induced by protons on the target nuclei  $^{64}\text{Ni}$ ,  $^{78}\text{Kr}$ , and  $^{86}\text{Sr}$ . The strong  $(p, n)$  channel is described well by the calculation. In the case of weaker channels some discrepancies occurred between the experimental and theoretical data, in particular for  $^{78}\text{Kr}$  as target. Regarding the  $(p, \alpha)$  process, an attempt was made to include direct three-nucleon pickup component. For the neutron deficient target nuclei  $^{78}\text{Kr}$  and  $^{86}\text{Sr}$  the direct reaction contribution to the  $(p, \alpha)$  cross section appears to be small, presumably due to large  $(p, n)$  thresholds. Inclusion of this component in the  $(p, \alpha)$  reaction on the neutron rich target nuclide  $^{64}\text{Ni}$ , however, led to a better agreement between the experimental and theoretical data.

PACS number(s): 24.60.Dr, 24.50.+g, 25.40.Hs

### I. INTRODUCTION

The emission of nucleons in the interactions of light projectiles with nuclei is generally described in terms of equilibrium and preequilibrium effects. The emission of  $\alpha$  and other complex particles, on the other hand, is difficult to formulate and may involve contributions from direct processes, populating low-lying levels of specific structure. Such contributions are mainly of interest in nuclear structure studies, but may also become significant in the case of activation cross section, especially when other mechanisms are suppressed, e.g., by  $Q$ -value and/or Coulomb barrier effects.

Smits and Siemssen [1] developed a semimicroscopic approach which allows the calculation of three-nucleon pickup cross sections in terms of spectroscopic factors of simpler reactions up to a normalization constant common to all final states. In several investigations on  $(p, \alpha)$  and  $(n, \alpha)$  processes concerning nuclear structure and reaction mechanism, Gadioli *et al.* showed that the aforementioned normalization constant is, to a good approximation, independent of the incident energy and changes little between neighboring nuclei (cf., e.g., Refs. [2,3] and other references quoted therein). Due to these properties the semimicroscopic approach is also of interest for calculating application oriented data. In the case of  $^{48}\text{Ti}(n, \alpha)^{45}\text{Ca}$  and  $^{50}\text{Ti}(n, \alpha)^{47}\text{Ca}$  reactions [4], for example, we showed recently that the reproduction of activation cross sections can be improved by considering a direct reaction component in addition to the compound

and precompound contributions. Now we chose to study the excitation functions of the  $(p, \alpha)$  reactions on  $^{64}\text{Ni}$ ,  $^{78}\text{Kr}$ , and  $^{86}\text{Sr}$ . The three isotopes occur at different distances from the line of stability of elements and are thus suitable for investigation of  $Q$ -value effects. Due to lack of spectroscopic information, however, an assessment of the direct  $\alpha$  component is expected to be more difficult than for the  $^{48,50}\text{Ti}(n, \alpha)$  reactions studied earlier.

### II. EXPERIMENT

Excitation functions were measured by the activation method. The details for the  $^{78}\text{Kr}(p, \alpha)^{75}\text{Br}$  reaction have already been given [5]. In brief, thin walled metal cylinders, filled with 99.4% enriched  $^{78}\text{Kr}$ , were irradiated in a row with a well-collimated beam of protons, and the radioactivity of the product nuclide  $^{75}\text{Br}$  was determined via  $\gamma$ -ray spectrometry. In studies on  $^{64}\text{Ni}(p, \alpha)^{61}\text{Co}$  and  $^{86}\text{Sr}(p, \alpha)^{83}\text{Rb}$  reactions the well-known stacked-foil technique, commonly used at Jülich (cf. Refs. [6–8]), was employed. Details of measurements are given below.

#### A. $^{64}\text{Ni}(p, \alpha)^{61}\text{Co}$ reaction

Thin samples were prepared by an electroplating method [7,8] and consisted of thin layers ( $\approx 1 \text{ mg cm}^{-2}$ ) of 95% enriched  $^{64}\text{Ni}$  on Au foils. Several stacks, each consisting of  $^{64}\text{Ni}$  samples, Cu monitor foils, and Al absorbers, were irradiated with the external beam of the Compact Cyclotron CV 28 of KFA Jülich for about 30 min at proton beam currents of 150–200 nA. The primary proton energies used were 18.7 and 14.9 MeV. The beam current was measured by a Faraday cup and was also monitored through the monitor reactions induced in

\*Deceased March 1995.

†On leave of absence from ATOMKI, Debrecen, Hungary.

$^{\text{nat}}\text{Cu}$  foils (cf. Refs. [9,10]).

The radioactivity of the  $^{64}\text{Ni}(p,\alpha)^{61}\text{Co}$  reaction product ( $T_{1/2} = 1.65$  h,  $E_\gamma = 67.4$  keV,  $I_\gamma = 84.7\%$ ) was determined using a thin high-purity Ge (HP Ge) detector with a Be window. The detector was coupled to an Ortec MCA plug-in card which was connected to an IBM-compatible PC-AT. The full widths at half maximum (FWHM) of the two  $\gamma$  rays of  $^{57}\text{Co}$  at 14.4 and 122 keV measured with the detector were 0.39 and 0.59 keV, respectively. The detector was thus ideally suited for counting  $^{61}\text{Co}$ . Nonetheless, the peak area analysis met with considerable difficulty due to the occurrence of the  $K\alpha_2$  and  $K\alpha_1$  x rays of Au and Pt (at 66.99 and 66.8 keV, respectively) in the vicinity of the 67.4 keV  $\gamma$  ray of  $^{61}\text{Co}$ . The Au and Pt x rays are emitted in the decay of Hg and Au radioisotopes formed via  $(p, xn)$  and  $(p, pxn)$  reactions on Au backing. We used a flexible  $\gamma$ -ray analysis program FGM [11] which calculates the peak areas of a doublet by a fitting method based on a weighted least squares regression algorithm. The peak areas determined from spectra taken at two different decay times agreed within 5%. Nevertheless, for a further check two other tests were performed.

(a) A few irradiated samples were counted on a 145  $\text{cm}^3$  HPGe detector and the weak 908.6 keV  $\gamma$  ray ( $I_\gamma = 3.7\%$ ) of  $^{61}\text{Co}$  was searched for. Due to the dominant  $^{64}\text{Cu}$  ( $T_{1/2} = 12.7$  h) and  $^{197}\text{Hg}$  ( $T_{1/2} = 64$  h) activities the peak area of  $^{61}\text{Co}$  could be obtained only with a large error. The value, however, agreed with that deduced via an analysis of the 67.4 keV  $\gamma$  ray within  $\pm 10\%$ .

(b) Four irradiated samples were processed chemically. Nickel was dissolved in dilute  $\text{HNO}_3$  and 20 mg each of copper and cobalt were added as carriers. Cobalt was separated via anion-exchange chromatography (cf. Ref. [12]) and counted on the thin HPGe detector described above. A clean peak at 67.4 keV was observed. There was some uncertainty in the gravimetric yield of the separated sample but the peak area agreed within  $\pm 10\%$  with the value obtained without chemical separation.

From the results of the three counting methods we assumed an error of 8–10% in the peak area analysis. The absolute activity was determined using the  $\gamma$ -ray abundance and the efficiency of the detector. Thereafter the cross section was calculated using the activation formula. The overall error was estimated as described in several earlier publications (cf. Refs. [5,7,8]); it amounted to between 12% and 15%.

### B. $^{86}\text{Sr}(p,\alpha)^{83}\text{Rb}$ reaction

For work on this reaction thin samples of  $^{86}\text{SrCO}_3$  ( $^{86}\text{Sr}$  enrichment 96.3%) were prepared by a sedimentation process [13]. A thin Cu foil (25  $\mu\text{m}$ ) was used as backing material and the thickness of the carbonate layer amounted to about 10  $\text{mg}/\text{cm}^2$ . The deposited layer was covered with a 25  $\mu\text{m}$  thick Al foil; each sample was thus in a sandwich form. Irradiations and beam current measurements were done as described above for the  $^{64}\text{Ni}(p,\alpha)$  reaction.

The radioactivity of the reaction product  $^{83}\text{Rb}$  ( $T_{1/2} = 86.2$  d,  $E_\gamma = 520$  keV,  $I_\gamma = 46\%$ ) was measured several months after the end of irradiation, i.e., after the decay of the shorter-lived radioisotopes. Due to the low level of activity involved, the counting time for each sample ranged between 1 and 5 d. Use was made of the large-sized HPGe detector (see above) and the peak area analysis was done using MAESTRO II MCA emulation software. The cross sections and their errors were obtained as described in several publications (cf. Refs. [5,7,8]). The error near the threshold of the reaction was high (up to 60%) due to relatively poor counting statistics. In general, however, the error was around 15%.

### III. NUCLEAR MODEL CALCULATIONS

The models and parameters were chosen as in our previous study on  $^{48,50}\text{Ti}(n,\alpha)$  activation cross sections [4]. The *compound nucleus evaporation* contribution was calculated taking into consideration angular momentum and parity conservation and—for completeness—also isospin effects. The latter were treated in the framework of a model proposed by Grimes *et al.* [14], assuming a mixing parameter  $\mu = 0.4$  based on the trend given by Harney, Weidenmüller, and Richter [15]. Isospin effects in proton induced reactions on  $N > Z$  targets favor  $(p, p')$  processes and reduce the emission of neutrons and  $\alpha$  particles. For the target nuclei considered here this reduction was rather moderate; it was of little importance regarding the agreement between experiment and calculations.

The particle transmission coefficients were derived from global optical potentials proposed by Rapaport, Kulkarni, and Finlay [16], Mani, Melkanoff, and Iori [17], and McFadden and Satchler [18] for neutrons, protons, and  $\alpha$  particles, respectively. The neutron potential is defined only for incident energies exceeding 7 MeV; below this limit we assumed an energy independent strength of the surface absorptive potential with the value prescribed at 7 MeV. The  $\alpha$  particle potential of Ref. [18] was slightly modified as described in Ref. [19]. These optical potentials for protons and  $\alpha$  particles were employed for the direct reaction calculations, too. For the  $\gamma$ -ray transmission coefficients we used a “generalized Lorentzian” in the case of the dominant  $E1$  and a “standard Lorentzian” in the case of  $M1$  and  $E2$  radiation (for details see Refs. [20,21]); the single particle model was applied for the less important multipole types  $M2$ ,  $E3$ , and  $M3$ .

The information on low-lying levels was taken from recent issues of the Nuclear Data Sheets [22]. The level densities were derived from the model of Kataria, Ramamurthy, and Kapoor [23] supplemented for lower excitation energies by a constant temperature formula (see Ref. [4] for more details). The level density parameters were determined by reproducing the number of low-lying levels and the average  $s$ -wave resonance spacing  $D_0$  compiled by Mughabghab, Divadeenam, and Holden [24]. Unfortunately, for most of the nuclei encountered in reactions considered here no information on  $D_0$  values is available since they are unstable. Therefore the

level density parameters for these nuclei had to be found by interpolation from neighboring nuclei. Though the level density model of Kataria *et al.* [23] is rather well suited for interpolations, since it explicitly accounts for shell effects, the level density of each of these nuclei is afflicted by considerable uncertainties, thereby affecting the calculated cross sections.

The *preequilibrium emission*—as in Ref. [4]—was treated in the framework of the exciton model, accounting for angular momentum as proposed by Shi Xiangjun, Gruppelaar, and Akkermans [25].  $\alpha$  particle emission rates were chosen according to the model of Milazzo-Colli and Braga-Marcazzan [26] with a preformation factor  $\phi = 0.25$ ; more details on the preequilibrium contributions can be found in Ref. [4].

*Direct reaction cross sections* were calculated with the distorted-wave method. Inelastic scattering populating low-lying collective levels were considered for all three target nuclei; the deformation parameters were taken from Ref. [22]. These cross sections reduce the combined compound and precompound contribution by a few percent.

For the  $^{64}\text{Ni}(p, \alpha)$  reaction we considered direct contributions to the low-lying levels in an analogous way as in Ref. [4]. The processes were described as pickup of a tritonlike cluster in the framework of the semimicroscopic model of Smits and Siemssen [1] under rather simple assumptions. For all final states the two neutrons were considered to be picked up from the  $1f_{5/2}$  shell model orbit and to form a pair coupled to angular momentum  $\bar{J} = 0$ , and so the spectroscopic factor for the two neutrons can be lumped into the normalization factor. The final states considered extend up to an excitation energy of 2.6 MeV; those were strongly populated in the  $^{64}\text{Ni}(p, \alpha)$  reaction [27] and in the proton pickup process  $^{62}\text{Ni}(d, ^3\text{He})$  [28]. For those states the proton is picked up from the  $1f_{7/2}$  orbit or the  $s$  and  $d$  orbits of the  $Z = 8-20$  major shell; the relevant spectroscopic factors for proton pickup were taken from Ref. [28]. The three-nucleon cluster bound states were generated in a Woods-Saxon potential with a reduced radius of 1.25 fm and a diffuseness of 0.60 fm. The distorted-wave calculations were performed in the zero-range approximation. The choice of the normalization constant is described in the next section.

For the  $^{78}\text{Kr}(p, \alpha)$  and  $^{86}\text{Sr}(p, \alpha)$  processes we neglected the direct reaction contributions for the following reasons (i) Spectroscopic information and absolute cross sections required for the normalization are not available. (ii) The combined contributions of compound nucleus evaporation and preequilibrium emission reproduce or even overpredict the  $(p, \alpha)$  activation cross section so that no meaningful assessment of the direct component is possible.

The calculations were performed with the codes MAURINA [29] and DWUCK4 [30] which are combined by suitable interface routines.

#### IV. RESULTS AND DISCUSSION

The experimental data on the  $^{78}\text{Kr}(p, \alpha)^{75}\text{Br}$  reaction were reported earlier [5]. The measured cross sections for

TABLE I. Measured cross sections of the  $^{64}\text{Ni}(p, \alpha)^{61}\text{Co}$  reaction.

Proton energy (MeV)	Cross section (mb)
5.04±0.60	0.02±0.003
6.63±0.55	0.62±0.09
7.80±0.52	1.48±0.19
8.26±0.51	1.98±0.25
8.41±0.50	1.76±0.23
9.26±0.48	3.44±0.44
9.60±0.47	3.95±0.50
10.38±0.44	5.09±0.65
10.72±0.43	6.58±0.84
11.25±0.42	8.75±1.10
11.77±0.40	10.17±1.37
12.02±0.40	11.80±1.85
12.62±0.39	10.84±1.37
12.73±0.37	11.37±1.44
13.23±0.36	12.78±1.61
13.52±0.36	14.02±1.45
14.12±0.33	14.52±1.83
14.30±0.33	14.87±1.87
14.80±0.32	15.00±1.60
15.26±0.31	16.28±2.05
15.46±0.29	17.23±2.16
16.53±0.26	18.69±2.34
17.56±0.23	17.35±2.18
18.55±0.20	17.97±2.25

the  $^{64}\text{Ni}(p, \alpha)^{61}\text{Co}$  and  $^{86}\text{Sr}(p, \alpha)^{83}\text{Rb}$  processes are given in Tables I and II, respectively. For both the reactions no data were available in the literature.

The results of nuclear model calculations are shown as curves in several diagrams (see below). Since we were mainly interested in investigating the applicability and predictive power of simple models, we did not attempt to improve the reproduction of the data by exploiting the uncertainties in the model parameters. For the same reason we compare, besides the  $(p, \alpha)$  activation cross sections under consideration, also experimental data on competing reactions with the results of model calculations.

TABLE II. Measured cross sections of the  $^{86}\text{Sr}(p, \alpha)^{83}\text{Rb}$  reaction.

Proton energy (MeV)	Cross section (mb)
7.82±0.52	0.25±0.13
8.71±0.55	0.19±0.07
9.91±0.48	0.32±0.22
10.69±0.44	0.54±0.32
11.74±0.40	2.38±0.62
12.43±0.40	2.75±0.73
13.38±0.38	3.98±0.70
14.01±0.36	4.13±1.06
14.89±0.32	4.54±0.53
15.49±0.29	5.65±0.68
16.29±0.27	5.54±0.68
16.85±0.25	9.57±1.20
17.63±0.23	7.27±1.12
18.16±0.22	14.66±1.82

### A. Protons on $^{64}\text{Ni}$

The experimental  $^{64}\text{Ni}(p, \alpha)^{61}\text{Co}$  activation cross sections are compared with the results of model calculations in Fig. 1. The solid curve describes the sum of compound nucleus evaporation and preequilibrium emission, and the dashed curve the sum of these processes as well as the direct component. For lack of independent experimental data we normalized the direct ( $p, \alpha$ ) contribution such that the sum of the three calculated contributions reproduced the experimental cross section at 15 MeV. The reproduction of the experimental excitation function was considerably improved through the inclusion of the direct component, which is illustrated on a linear scale in Fig. 2, and is compared with the statistical contribution. In view of the different energy dependences of the calculated compound and direct contributions, and considering the fact that a change in the level density parameters for the products  $^{61}\text{Co}$  and  $^{64}\text{Cu}$  did not lead to a satisfactory reproduction of the measured ( $p, \alpha$ ) excitation function, we found the necessity of inclusion of a direct contribution. However, it must be emphasized that the absolute magnitude of the direct ( $p, \alpha$ ) contribution is strongly affected by the previously mentioned uncertainties in the compound and precompound components. The experimental activation cross sections for the competing  $^{64}\text{Ni}(p, n)^{64}\text{Cu}$  reaction (cf. Ref. [8]) are compared with the results of model calculations in Fig. 3; here the solid and the dashed curves coincide. The reproduction of the data is not excellent but, apart from the high-energy end of the excitation function, quite reasonable.

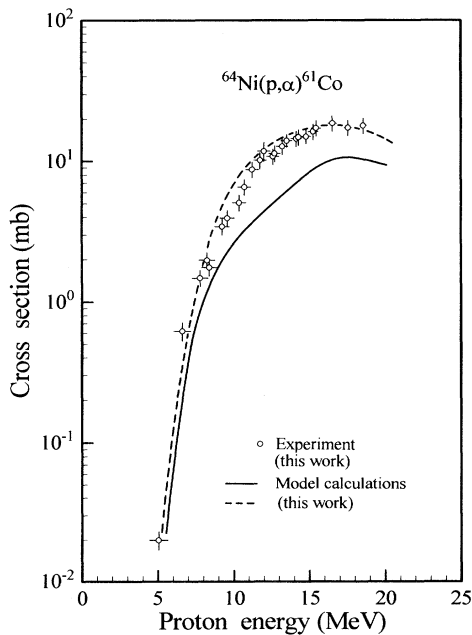


FIG. 1. Measured and calculated cross sections for the  $^{64}\text{Ni}(p, \alpha)^{61}\text{Co}$  process. The solid curve describes the sum of the compound nucleus evaporation and preequilibrium emission. The dashed curve includes an additional direct pickup component.

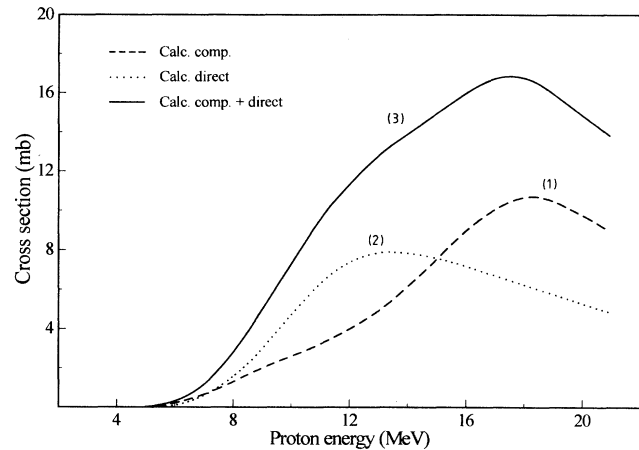


FIG. 2. Comparison of energy dependence of compound nucleus plus preequilibrium model component (1) and direct component (2) to the  $^{64}\text{Ni}(p, \alpha)^{61}\text{Co}$  cross section. The solid line (3) represents the sum of the two components and hence corresponds to the dashed line in Fig. 1.

### B. Protons on $^{78}\text{Kr}$

The  $^{78}\text{Kr}(p, \alpha)^{75}\text{Br}$  activation cross sections measured recently [5] are compared with the results of model calculations in Fig. 4. Only compound and preequilibrium effects were considered. Below 16 MeV the experimental data and calculations disagree, there being a shift of several MeV between the experimental and theoretical excitation functions. Since in the experimental work the

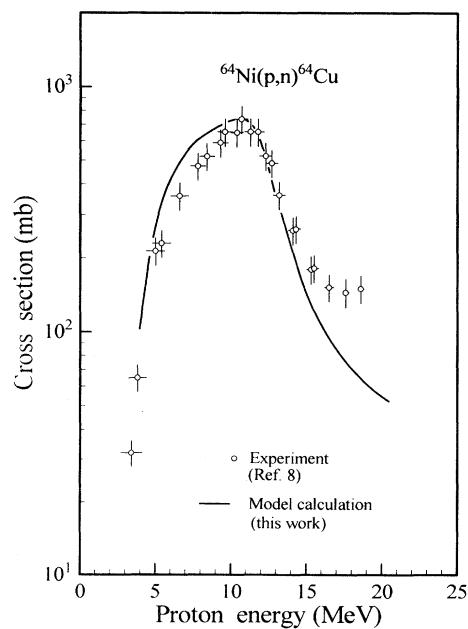


FIG. 3. Measured and calculated cross sections for the  $^{64}\text{Ni}(p, n)^{64}\text{Cu}$  reaction. The calculation took into account only the compound nucleus evaporation and preequilibrium processes.

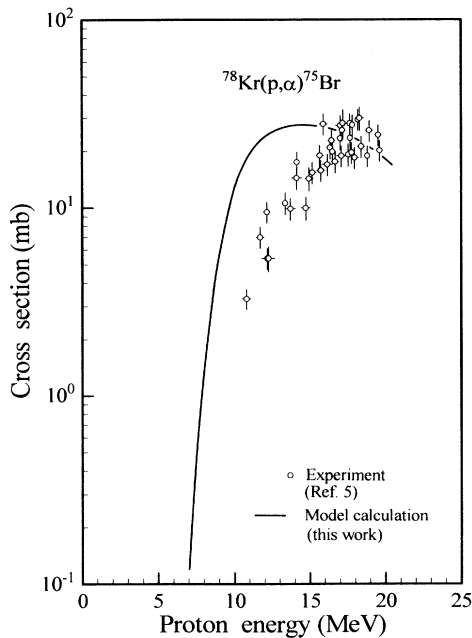


FIG. 4. Measured and calculated cross sections for the  $^{78}\text{Kr}(p, \alpha)^{75}\text{Br}$  process; other details are the same as for Fig. 3.

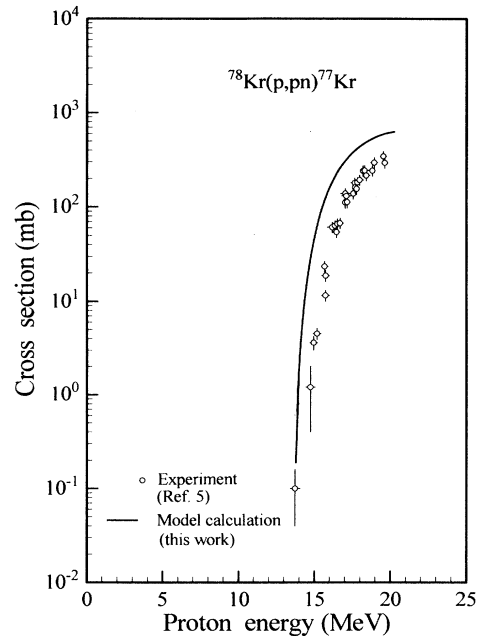


FIG. 5. Measured and calculated cross sections for the  $^{78}\text{Kr}(p, np)^{77}\text{Kr}$  process; other details are the same as for Fig. 3.

incident energy was carefully checked [5], the discrepancy is not due to an error in the energy scale. No substantial improvement could be achieved in this energy region by employing other optical potentials, other level density models, or by exploiting the considerable uncertainties in the interpolated resonance spacings. The shape of the rising part of the  $(p, \alpha)$  excitation function is mainly determined by the  $Q$  value and the Coulomb barrier and is therefore rather insensitive to variations in the model parameters. Figure 4 also illustrates that an improvement in the reproduction of the experimental data by an additional direct reaction contribution is not very plausible. As displayed in Figs. 5 and 6 the model calculations also overpredict the experimental  $^{78}\text{Kr}(p, np)^{77}\text{Kr}$  and  $^{78}\text{Kr}(p, x)^{77}\text{Br}$  cross sections [5]; the latter includes both direct formation through the  $(p, 2p)$  reaction as well as via the decay of  $^{77}\text{Kr}$ . Figure 6 therefore represents the sum of the  $(p, 2p)$  and  $(p, np)$  cross sections. While the experimental  $(p, np)$  and  $(p, x)$  cross sections practically agree with each other [5], the calculations predict an appreciable  $(p, 2p)$  cross section [at  $E_p = 18$  MeV, e.g., about 30% of the  $(p, x)$  cross section]. This is presumably due to the rather high  $(p, n)$  threshold of 7.84 MeV, resulting in an enhancement of proton emission at the equilibrium and preequilibrium stage.

### C. Protons on $^{86}\text{Sr}$

In Fig. 7 we compare the experimental  $^{86}\text{Sr}(p, \alpha)^{83}\text{Rb}$  activation cross sections with the results of nuclear model calculations incorporating only compound nucleus evaporation and preequilibrium emission. The agreement

is quite good and so, for reasons mentioned above, we did not attempt to add a direct reaction contribution. The experimental cross sections for the competing  $^{86}\text{Sr}(p, n)^{86}\text{Y}$  reaction [13] are somewhat larger than the results of the model calculations as shown in Fig. 8; however, the difference cannot be considered as a serious discrepancy.

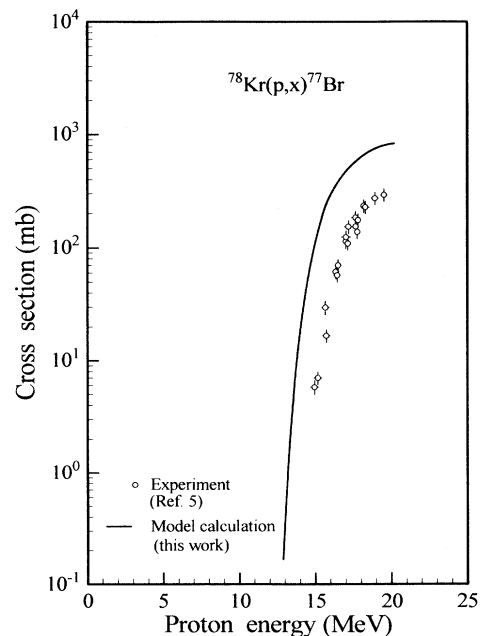


FIG. 6. Measured and calculated cross sections for the  $^{78}\text{Kr}(p, x)^{77}\text{Br}$  process; other details are the same as for Fig. 3.

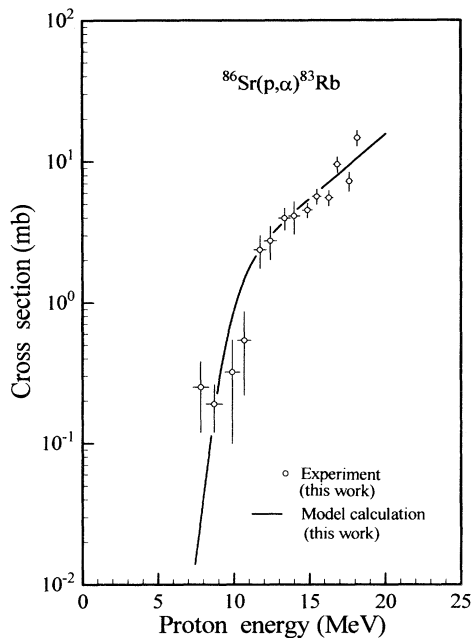


FIG. 7. Measured and calculated cross sections for the  $^{86}\text{Sr}(p, \alpha)^{83}\text{Rb}$  process; other details are the same as for Fig. 3.

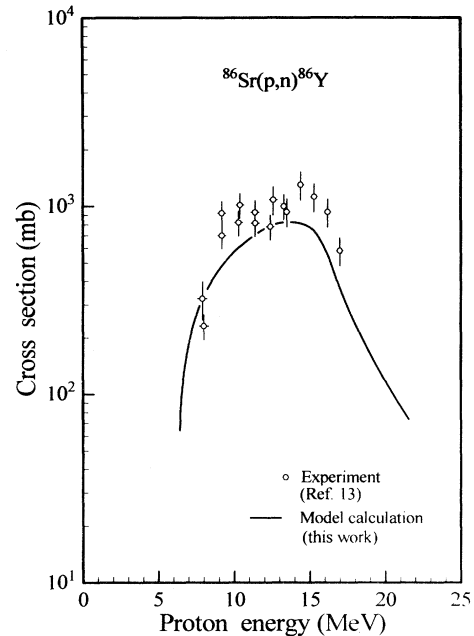


FIG. 8. Measured and calculated cross sections for the  $^{86}\text{Sr}(p, n)^{86}\text{Y}$  reaction; other details are the same as for Fig. 3.

## V. CONCLUSIONS

The combined evaporation and preequilibrium contribution underpredicts the experimental  $(p, \alpha)$  activation cross sections above 9 MeV only in the case of  $^{64}\text{Ni}$  as target. For the targets  $^{78}\text{Kr}$  and  $^{86}\text{Sr}$  the effect of a direct reaction component in the  $(p, \alpha)$  activation cross section seems to be smaller. This may be due to the high thresholds of  $(p, n)$  reactions on the neutron deficient target nuclei  $^{78}\text{Kr}$  (7.84 MeV) and  $^{86}\text{Sr}$  (6.05 MeV). Presumably, for these target nuclei the statistical  $(p, \alpha)$  contribution is enhanced compared to that for the neutron rich target nucleus  $^{64}\text{Ni}$  which has a  $(p, n)$  threshold of 2.46 MeV. However, more quantitative conclusions require absolute cross sections for  $\alpha$  groups populating levels for which the direct mechanism dominates.

## ACKNOWLEDGMENTS

The Jülich authors thank Professor G. Stöcklin for his active support of the experimental program. The help of Brigitte Strohmaier in clarifying some points regarding the model calculations, after the death of M. Uhl, is gratefully acknowledged. Acknowledgment is also made to the crew of the Jülich compact cyclotron for irradiations and F. Sudbrock and W. Schade for experimental assistance. F. Szelecsényi is grateful to the International Atomic Energy Agency, Vienna, Austria for financial support. The model calculations were performed on an IBM 3090-400E computer installed at the University of Vienna in the frame of the European Academic Supercomputing Initiative (EASI) of IBM Corporation.

- 
- [1] J. W. Smits and R. H. Siemssen, Nucl. Phys. **A261**, 385 (1975).  
 [2] E. Gadioli, E. Gadioli Erba, P. Guazzoni, M. Luinetti, L. Zetta, G. P. A. Berg, J. Meissburger, D. Paul, D. Prashuhn, J. G. M. Roemer, and P. von Rossen, Z. Phys. A **325**, 61 (1986).  
 [3] E. Gadioli, S. Mattioli, W. Augustyniak, L. Glowacka, M. Jaskola, J. Turkiewicz, and A. Chiadli, Phys. Rev. C **43**, 1932 (1991).  
 [4] S. M. Qaim, M. Uhl, N. I. Molla, and H. Liskien, Phys. Rev. C **46**, 1398 (1992).  
 [5] F. Tárkányi, Z. Kovács, and S. M. Qaim, Appl. Radiat. Isotopes **44**, 1105 (1993).  
 [6] S. M. Qaim, G. Stöcklin, and R. Weinreich, Int. J. Appl. Radiat. Isotopes **28**, 947 (1977).  
 [7] H. Piel, S. M. Qaim, and G. Stöcklin, Radiochim. Acta **57**, 1 (1992).  
 [8] F. Szelecsényi, G. Blessing, and S. M. Qaim, Appl. Radiat. Isotopes **44**, 575 (1993).  
 [9] P. Kopecký, Int. J. Appl. Radiat. Isotopes **36**, 657 (1985).  
 [10] O. Schwerer and K. Okamoto, IAEA Report No. INDC (NDS)-218/GZ, Vienna, Austria, 1989 (unpublished).  
 [11] G. Székely, Comput. Phys. Commun. **34**, 313 (1985).  
 [12] S. M. Qaim, R. Wölffe, and G. Stöcklin, J. Radioanal. Chem. **30**, 35 (1976).  
 [13] F. Rösch, S. M. Qaim, and G. Stöcklin, Radiochim. Acta **61**, 1 (1993).  
 [14] S. M. Grimes, J. D. Anderson, A. K. Kerman, and C.

- Wong, Phys. Rev. C **5**, 85 (1972).
- [15] H. L. Harney, H. A. Weidenmüller, and A. Richter, Phys. Rev. C **16**, 1774 (1977).
- [16] J. Rapaport, V. Kulkarni, and R. W. Finlay, Nucl. Phys. **A330**, 15 (1979).
- [17] G. S. Mani, M. A. Melkanoff, and I. Iori, Report No. CEA-2379, 1963 (unpublished).
- [18] L. McFadden and G. R. Satchler, Nucl. Phys. **84**, 177 (1966).
- [19] M. Uhl, H. Gruppelaar, H. A. J. van der Kamp, J. Kopecký, and D. Nierop, in *Proceedings of the International Conference on Nuclear Data for Science and Technology*, Jülich, Germany, 1991, edited by S. M. Qaim (Springer-Verlag, Berlin, 1992), p. 924.
- [20] J. Kopecký and M. Uhl, Phys. Rev. C **41**, 1941 (1990).
- [21] J. Kopecký, M. Uhl, and R. E. Chrien, Phys. Rev. C **47**, 312 (1993).
- [22] B. Singh, Nucl. Data Sheets **62**, 603 (1991); M. M. King, *ibid.* **64**, 815 (1992); **69**, 1 (1993); Zhou Chunmai, *ibid.* **67**, 271 (1992); S. Rab, *ibid.* **63**, 1 (1991); A. R. Farhan, Shaheen Rab, and B. Singh, *ibid.* **57**, 223 (1989); A. R. Farhan and S. Rab, *ibid.* **60**, 735 (1990); B. Singh and D. A. Viggars, *ibid.* **51**, 225 (1987); H.-W. Müller and J. W. Tepel, *ibid.* **54**, 527 (1988); H. Sievers, *ibid.* **62**, 271 (1991); E. Browne, *ibid.* **66**, 281 (1992); H.-W. Müller, *ibid.* **50**, 1 (1987).
- [23] S. K. Kataria, V. S. Ramamurthy, and S. S. Kapoor, Phys. Rev. C **18**, 459 (1978).
- [24] S. F. Mughabghab, M. Divadeenam, and N. E. Holden, *Neutron Cross Sections* (Academic, New York, 1981), Vol. 1, Part A.
- [25] Shi Xiangjun, J. Gruppelaar, and J. M. Akkermans, Nucl. Phys. **A466**, 333 (1987).
- [26] L. Milazzo-Colli and G. Braga-Marcuzzan, Nucl. Phys. **A210**, 297 (1973).
- [27] J. W. Smits, R. H. Siemssen, S. Y. Van der Werf, and A. Van der Woude, Nucl. Phys. **A319**, 29 (1979).
- [28] A. Marinov, W. Oelert, S. Gopal, G. P. A. Berg, J. Bojowald, W. Hürlimann, I. Katayama, S. A. Martin, C. Mayer-Böricke, J. Meissburger, J. G. M. Römer, M. Rogge, J. L. Tain, P. Turek, L. Zemlo, R. B. M. Mooy, P. W. M. Glaudemans, S. Brant, V. Paar, M. Vouk, and V. Lopac, Nucl. Phys. **A431**, 317 (1984).
- [29] M. Uhl (unpublished).
- [30] P. D. Kunz (unpublished).